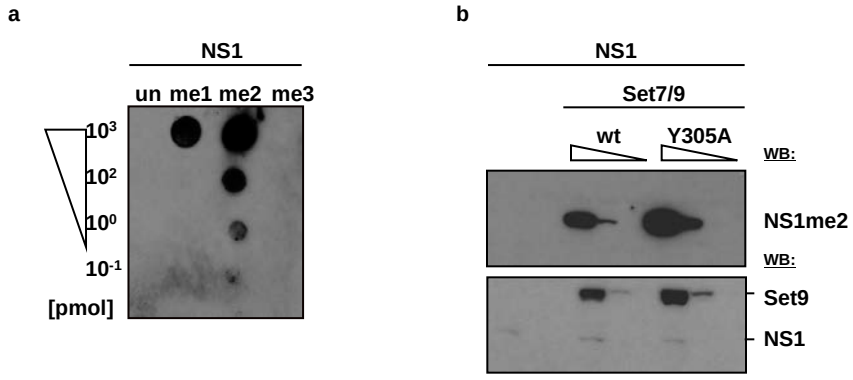


**Supplementary Fig. 1. Characterization of the K229 methyl-specific anti-NS1 antibodies. a)** Characterization of the K229 methyl-specific anti-NS1 antibodies. Unmodified (un), or synthetically methylated (K229me1, me2 or me3) NS1 peptides were serially diluted at indicated concentrations and spotted on a nitrocellulose filter. The binding specificity was tested by dot-blot analysis using affinity purified methyl-specific rabbit NS1 antibody. The results show the specificity of the NS1K229 di-methyl specific antibody (anti-NS1me2). **b)** The anti-NS1me2 antibody recognizes full-length GST-NS1 fusion protein pre-methylated *in vitro* by Set7/9 methyltransferase. The GST-NS1 protein was incubated *in vitro* with the wild-type or mutant (Y305A) Set7/9, which favors substrate di-methylation. Unmodified NS1 was incubated with serially diluted Set7/9 protein and separated by PAGE. The NS1 methylation was revealed by Western blotting with anti-NS1me2 antibody (upper panel). The amount of Set7/9 and GST-NS1 in the reaction mixture were determined by Western blotting using the corresponding antibodies.

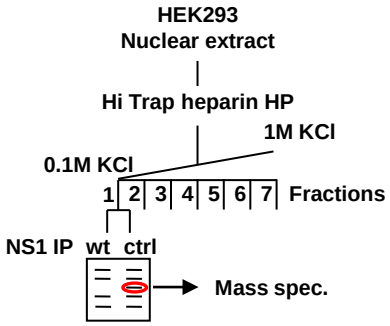


| Protein | Cellular Localization | Function |
|---|---|---|
| CHD1 | Nucleus | Co-transcriptional events |
| SMARCAL1 | Nucleus | Co-transcriptional events |
| CDC73 | Nucleus | Co-transcriptional events |
| RPA1 | Nucleolus | rDNA transcription |
| NOP56 | Nucleolus | Ribosome biogenesis |
| PRPF6 | Nucleus | Splicing |
| PARP1 | Nucleus | Protein modification |
| MATR3 | Matrix | Transcription (inferred) |
| EIF2C | Cytoplasm | Protein synthesis |
| EIF2B | Cytoplasm | Protein synthesis |
| EIF3D | Cytoplasm | Protein synthesis |
| EIF3G | Cytoplasm | Protein synthesis |
| WDR18 | Unknown | Unknown |
| C22ORF28 | Unknown | Unknown |

**Supplementary Fig. 2. Identification of NS1 “tail” interacting proteins in nuclear extracts.** The scheme of affinity purification of NS1 “tail”-binding nuclear proteins (left panel) and the list of identified proteins (right panel) are shown. NS1 binding proteins were identified by affinity purification of HEK293 nuclear extracts and NS1 bound proteins were separated by PAGE and visualized by colloidal coomassie staining. Proteins that displayed differential binding to the NS1 "tail" and scrambled control peptides were extracted from the gel and analyzed by mass spectrometry. The proteins that were identified with >95% accuracy are shown.

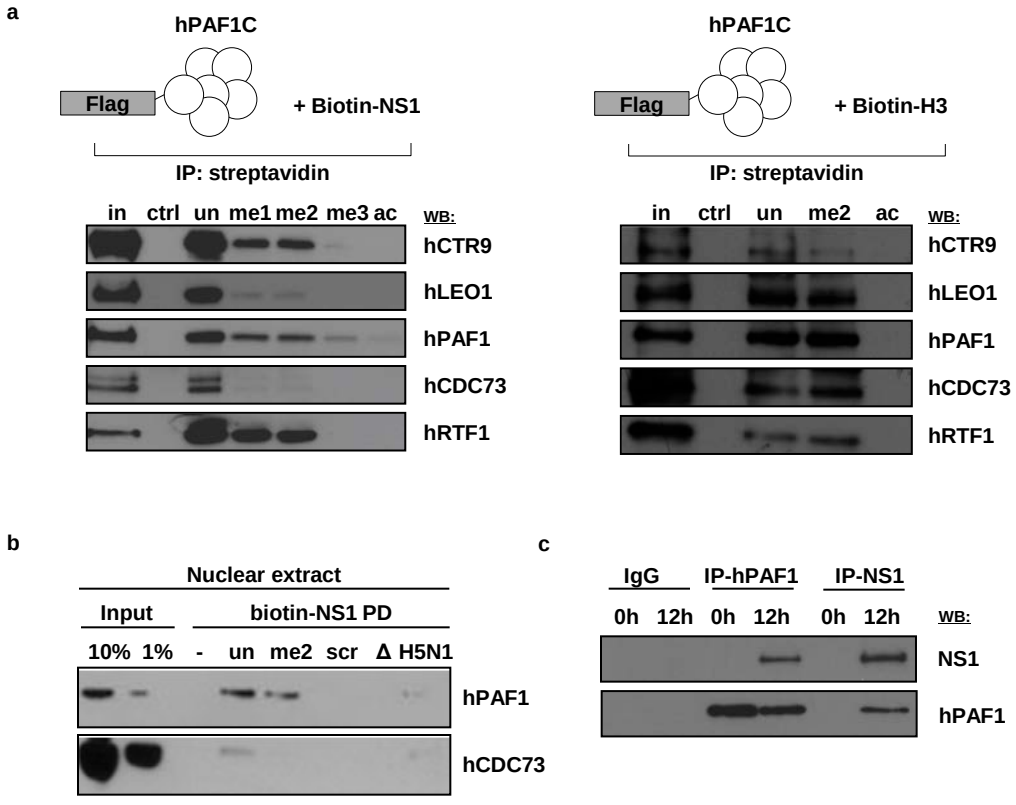


**Supplementary Fig. 3. NS1 "tail" and histone H3 peptides bind to recombinant hPAF1C. a)** Binding of NS1 (left) and H3 (right) peptides to recombinant hPAF1 complex. The recombinant hPAF1C was prepared as described[36] and incubated with the indicated NS1 or histone H3 peptides. The presence of the individual hPAF1C components in the peptide-bound fraction has been determined by Western blotting. **b)** NS1 associates with hPAF1C components in a sequence and modification-specific fashion. Nuclear extracts of A549 cells were incubated with the indicated unmodified or modified biotinylated NS1 peptides (220-230) and the presence of the peptide-bound hPAF1 or parafibromin proteins have been tested by Western blotting using corresponding antibodies. **c)** NS1 interacts with hPAF1 in the influenza infected cells. NS1 or hPAF1 were immunoprecipitated from cross-linked extracts of uninfected (0h) or infected (12h) A549 cells. The presence of hPAF1 or NS1 in the NS1 or hPAF1 precipitates, respectively, has been tested by Western blotting with specific antibodies. Treatment of cell extracts with control IgG shows absence of non-specific NS1 or hPAF1 precipitation.

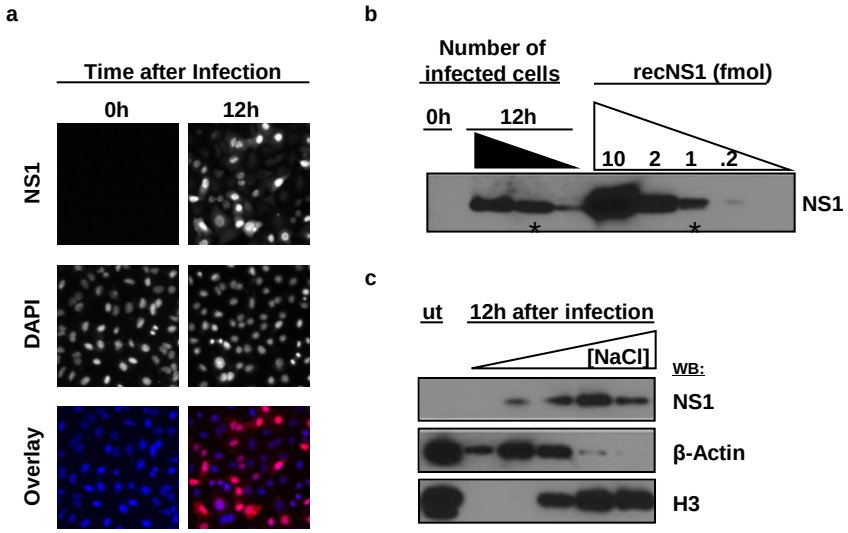


**Supplementary Fig. 4. Nuclear localization and expression of NS1 protein in infected cells**. **a)** Immunostained NS1 (red) co-localizes with DAPI-positive (blue) nuclei in A549 cells at 12h after infection. **b)** The amounts of NS1 in serially diluted nuclear extracts of A549 cells were determined by Western blotting and compared to defined amounts of recombinant NS1. The amount of NS1 protein per cell was calculated based on Avogadro's equation ($N_A = N/n$). **c)** The NaCl-elution profiles of NS1, β-actin and histone H3 are shown. The amount of indicated proteins in eluates was measured by Western blotting.

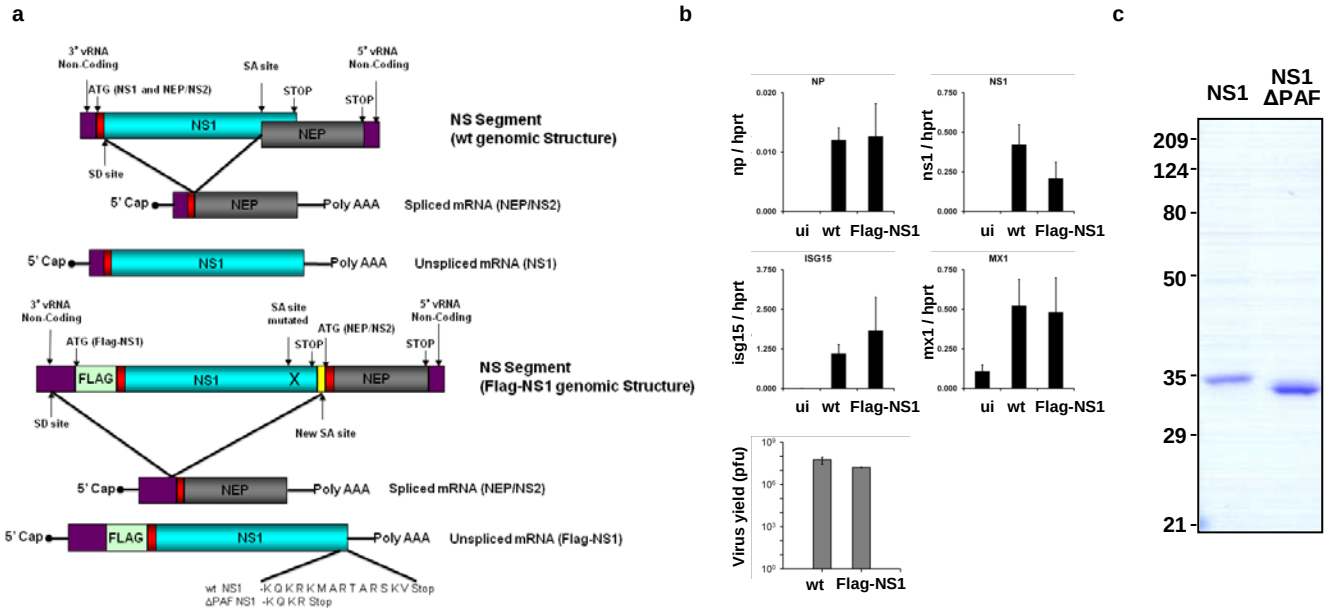


**Supplementary Fig. 5. Generation of reagents to study the function of the NS1 "histone mimic". a)** Generation of Flag-tagged NS1 virus. Schematic representation of the genomic structure of the NS segment of wild-type Influenza A virus and the strategy for the generation of the Flag-NS1 expressing influenza virus. Mutation of the splice acceptor site of the NS segment enables selective Flag-tagging of NS1. SD, SA splice donor or acceptor sites, respectively. **b)** Flag-NS1 recombinant virus supports infection and replication. A549 cells were infected with the wild-type or recombinant influenza virus that expresses Flag-tagged NS1. The virus functionality in single-cycle experiments was determined by expression of the viral nucleoprotein (NP) and NS1 in infected A549 cells (upper panel), by degree of up-regulation of the ISG15 and MX1 virus-induced genes in infected cells (middle panel) or yields of viruses propagated in MDCK cells (lower panel). **c)** Purification of the recombinant NS1. The wild-type full-length (NS1) and truncated NS1 (NS1ΔPAF) proteins were purified from baculovirus infected SF9 cells to maximum homogeneity as defined by coomassie staining following PAGE.

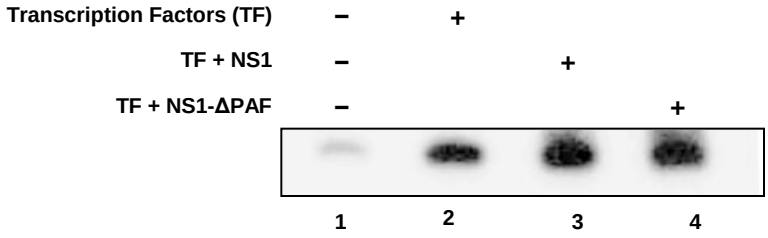


**Supplementary Fig. 6. NS1 does not affect transcription of non-chromatinized DNA template in vitro.** The 'naked' DNA template was incubated in the presence of transcription factors[62,63] and the full-length NS1 protein (NS1) or NS1 without the hPAF1 binding sequence (NS1-ΔPAF) under the same conditions described in Fig. 4. Autoradiography of the incorporated radioactive nucleotide in the reaction product is shown.

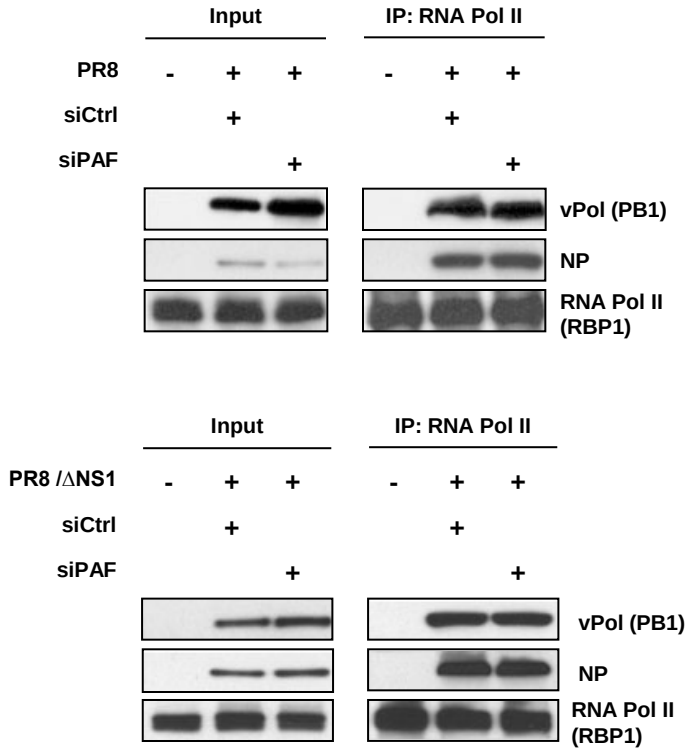


**Supplementary Fig. 7. hPAF1 does not control interaction between influenza RNA polymerase and cellular RNA Pol II.** A549 cells were treated with control (siCtrl) or hPAF1 specific (siPAF) siRNAs followed by infection with the wild-type (PR8) (upper panel) or NS1 deficient (PR8/ΔNS1) (lower panel) viruses. The interaction between viral RNA polymerase and cellular RNA Pol II was assessed by Western blotting analysis of viral polymerase (PB1), the viral polymerase-associated protein NP (NP) and the cellular RNA Pol II (RBP1) in immunoprecipates generated using anti-RNA Pol II antibody.

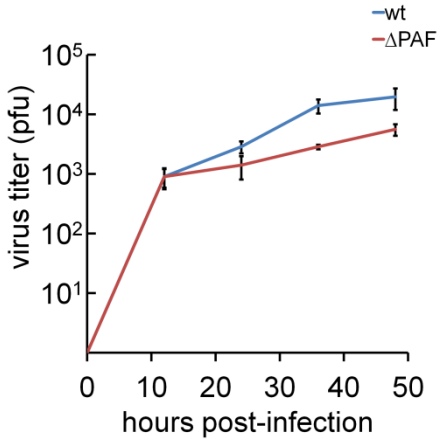


**Supplementary Fig. 8. The hPAF1 binding sequence in NS1 regulates influenza virulence.** A549 cells were infected with Flag-NS1 virus that carries wild-type (wt) or a truncated (220-230aa) version of the NS1 (ΔPAF). Virus-containing supernatants were collected at defined time points post-infection, serially diluted and incubated on confluent layers of MDCK cells. Viral titers were determined by enumerating plaque forming units on the infected MDCK cell layers. Shown is the average of 3 independent experiments with error bars representing the S.E.M.

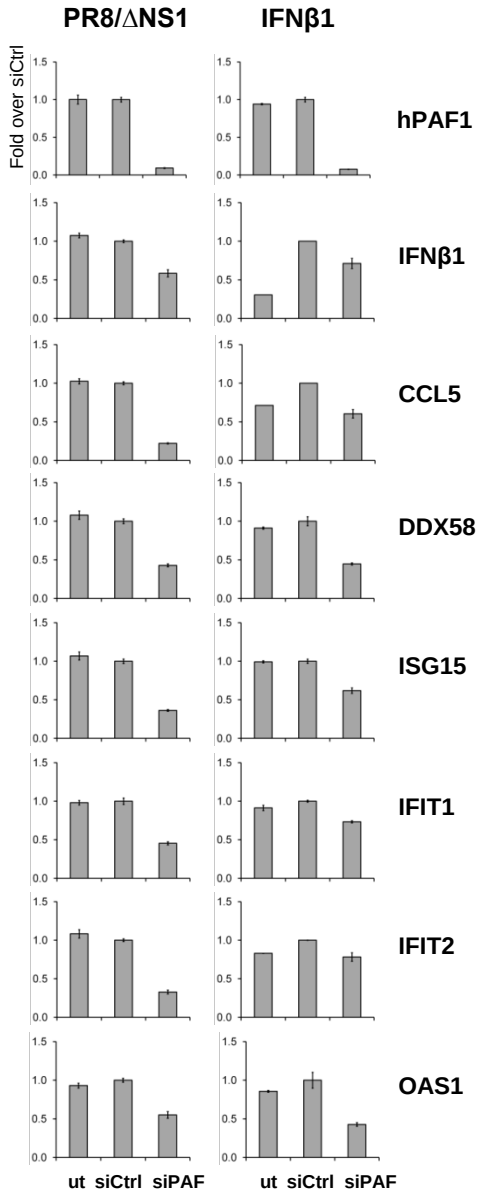


**Supplementary Fig. 9. hPAF1 deficiency suppresses up-regulation of the PR8/ΔNS1 and interferon beta (IFNβ1)-inducible genes.** The fold difference between levels of hPAF1 mRNA (upper panel) and indicated virus- or IFNβ1- induced mRNA up-regulation were measured by quantitative real time PCR of RNA isolated from infected (left panel) or IFNβ1-treated A549 cells (right panel) that were either not transfected (ut) or transfected with control (siCtrl) or hPAF1 (siPAF) specific siRNAs.

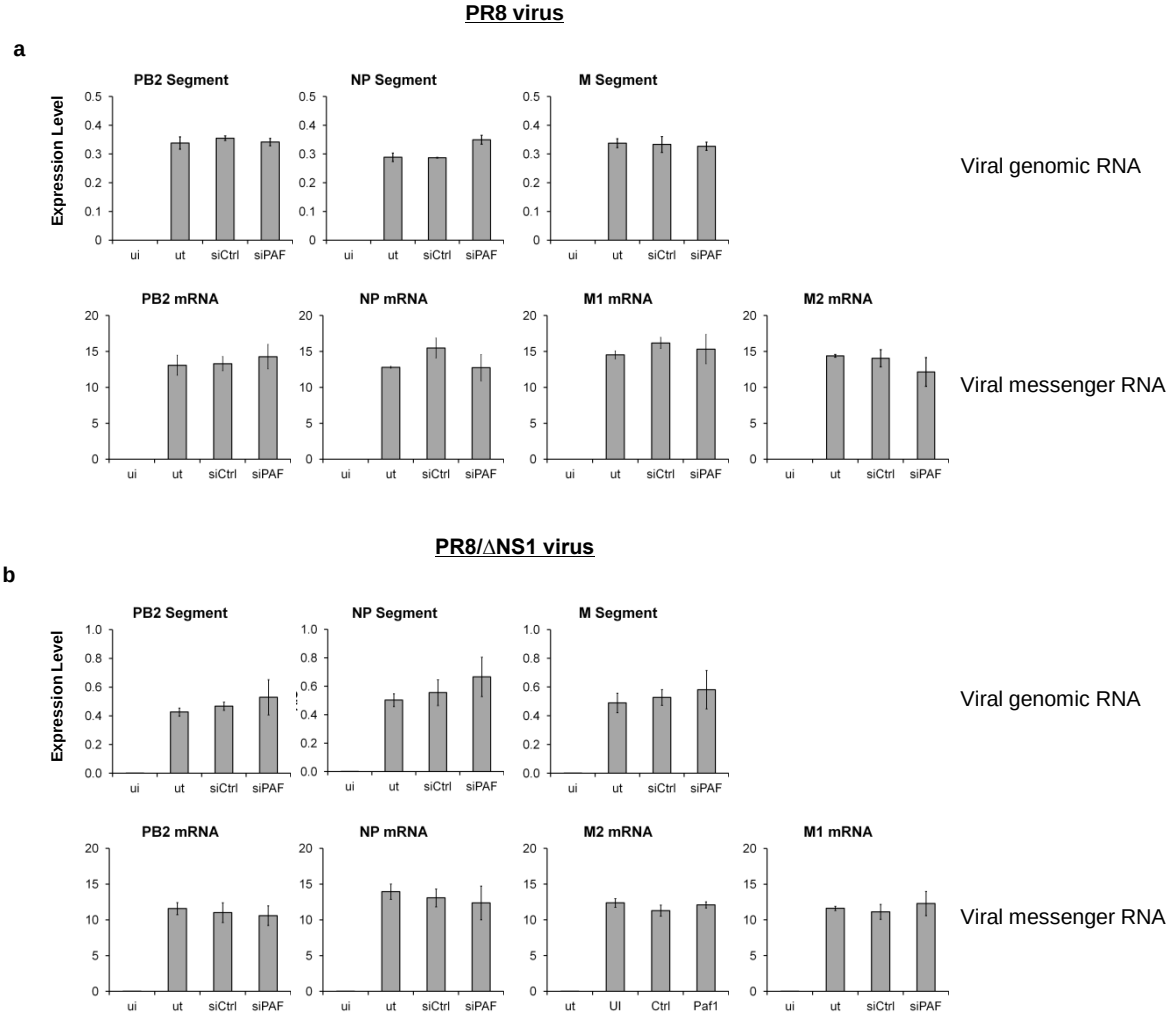


**Supplementary Fig. 11. hPAF1 does not control production of viral RNAs in influenza infected cells .** The levels of the indicated influenza genomic (upper panel) or messenger RNAs (lower panel) were measured by qPCR analysis of RNA derived either from uninfected (ui), hPAF1-deficient (siPAF1) or control (siCtrl) A549 cells infected with PR8 **(a)** or PR8/ΔNS1 **(b)** viruses. Data are representative of 3 independent experiments. Error bars represent the S.E.M.

**Influenza/H1N1**

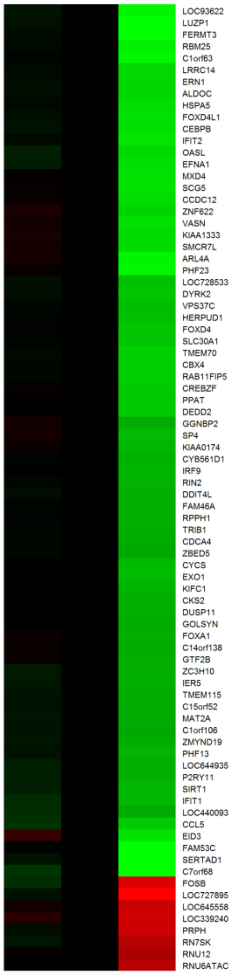


| Category | p-value |
|---|---|
| Gene Expression | 3.52E-07 |
| Cell Cycle | 2.98E-05 |
| Cellular Function | 4.57E-05 |
| Cell Death | 6.29E-05 |
| Lipid Metabolism | 2.13E-04 |

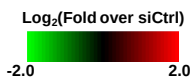


**VSV**

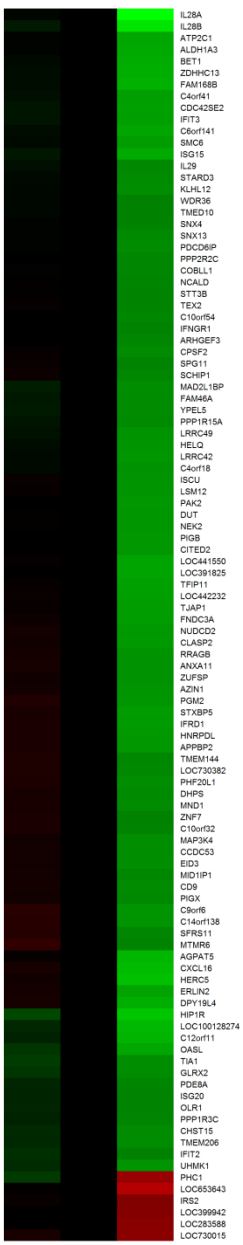


| Category | p-value |
|---|---|
| Infectious Disease | 1.9E-06 |
| Post-Translational | 0.00021 |
| Protein Folding | 0.00021 |
| Cell Death | 0.00075 |
| Cell-To-Cell Signaling | 0.00136 |

**Poly(I:C)**

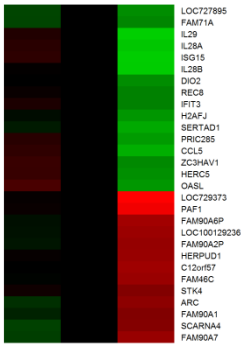


| Category | p-value |
|---|---|
| Infectious Disease | 2.14E-08 |
| Immune Cell Trafficking | 2.24E-06 |
| Inflammatory Response | 2.24E-06 |
| Cellular Development | 3.72E-06 |
| Antimicrobial Response | 9.58E-06 |

**Supplementary Fig. 11. hPAF1C controls antiviral gene expression in response to various stimuli.** The expression levels of antiviral genes were measured by microarray analysis of RNA isolated from wild-type influenza H1N1 (left panel), vesicular stomatitis virus (VSV) (middle panel) or Poly(I:C) treated (right panel) A549 cells that were either not transfected (ut) or transfected with control (siCtrl) or hPAF1 (siPAF) specific siRNAs. The tables show the top five functional categories of the siPAF affected genes as identified by IPA.

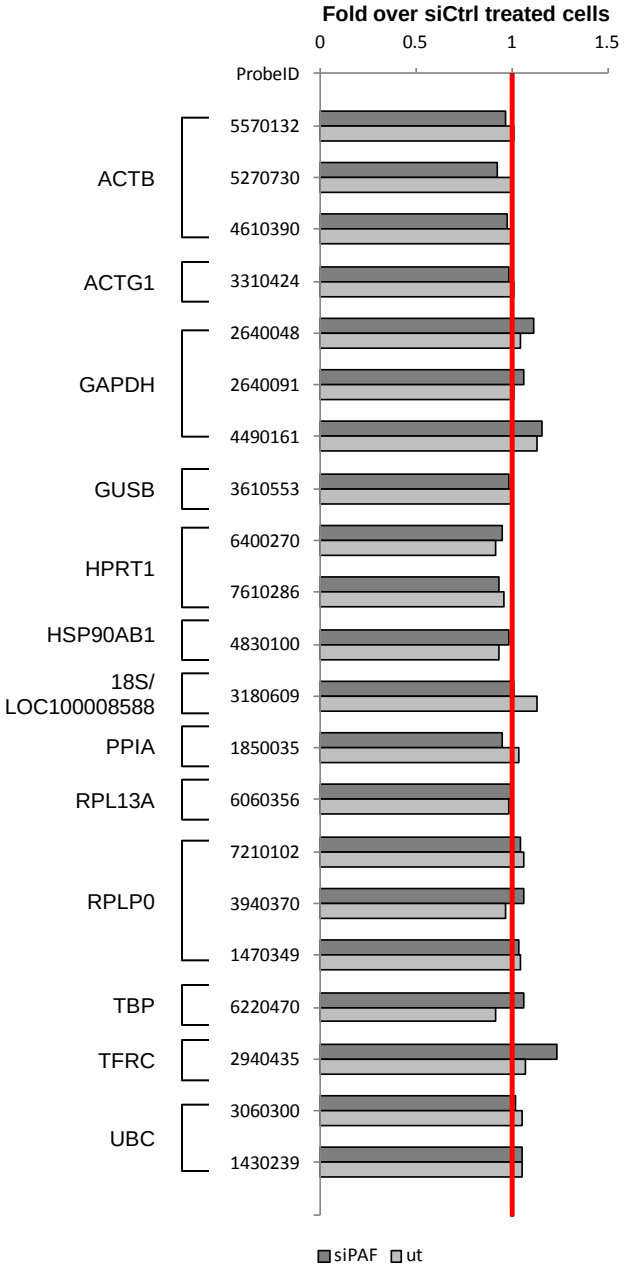


**Supplementary Fig. 12. hPAF1 is not essential for housekeeping gene expression.** Expression levels of indicated housekeeping genes were determined by microarray analysis of RNA derived from un-transfected (ut), siPAF or siCtrl transfected cells. Results for individual probesets are shown for genes that are represented by multiple probesets on the microarray.

**Supplementary Methods:**

**Cells, viruses**

A549 and Madin–Darby canine kidney (MDCK) cells were obtained from the American Type Culture Collection (ATCC) and were maintained in Dulbecco's minimal essential medium (DMEM) (Gibco, Invitrogen) supplemented with 2mM Glutamine (Gibco, Invitrogen), 10% Fetal Bovine Serum (Hyclone) and penicillin-streptomycin (Gibco, Invitrogen). The A/Wyoming/3/2003 (H3N2), A/Puerto Rico/8/1934 (H1N1) viruses and the Flag-NS1 strains were propagated on MDCK cells. The A/Puerto Rico/8/1934(ΔNS1) (PR8/ΔNS1) virus was propagated in NS1-expressing MDCK cells. Vesicular stomatitis virus (VSV) (Indiana strain) was propagated in BHK cells.

**Virus Growth Curves and Plaque Assays**

Confluent A549 cells were infected at a multiplicity of infection (MOI) of 0.01. Following infection, cells were maintained in DMEM containing 0.3% Bovine Serum Albumin (BSA) and 0.4 μg/ml of tosylsulfonyl phenylalanyl chloromethyl ketone (TPCK)-treated trypsin (Sigma). At the indicated time post infection, cell culture supernatants were collected. Viral titers at each time point were then quantified by plaque assays on MDCK cells.

For quantification of virus, dilutions of viral stocks or culture supernatants of the infected cells were adsorbed for 1 hour at room temperature onto layers of confluent MDCK cells. The infected MDCK cells were then overlaid with a 2 ml solution of DMEM containing 0.3% BSA, 25mM HEPES buffer (Gibco, Invitrogen), 2mM Glutamine (Gibco, Invitrogen), penicillin-streptomycin (Gibco, Invitrogen), 1 μg/mL TPCK-trypsin and 1% agar (LP0028, Oxoid). Plates

were then incubated 48 to 72 hours until plaques could be observed. Plaques were then fixed in a solution of 7% formaldehyde, before being visualized by crystal violet staining.

**Generation of Flag-NS1 viruses**

The NS1 and NEP ORF share a common N-terminal sequence. To attach the Flag tag specifically to NS1, the NS segment was modified as follows. The first 90 nucleotides of the 3'vRNA, with all the ATG start codons deleted, served as the 3' vRNA packaging signal. The endogenous splice donor site for NEP was left unchanged. The 3'vRNA packaging signal was followed by the 3XFlag sequence (MDYKDHDGDYKDHDIDYKDDDDK) and the NS1 ORF with stop codon. Two silent mutations in the endogenous splice acceptor site in the NS1 ORF (TTCCAGGACATA) were introduced to prevent splicing at this site (TTCCCGGGCATA) as described previously[51]. The Flag-NS1 ORF was followed by a new splice acceptor site that corresponds to the 459-527 nucleotides of the wild type NS segment, and the entire NEP-ORF with ATG. In this design, the 3XFlag-NS1 and NEP are generated from the unspliced or spliced mRNAs, accordingly. The deletion of the hPAF1 binding sequence was generated by introducing a stop codon after amino-acid 220 of the NS1 coding sequence. The modified NS segments were generated using fusion PCR and cloned into a pDZ vector using SapI restriction sites [52]. Flag-NS1 viruses were generated using reverse genetics system [53]. The sequence of the NS segment in the Flag-NS1 viruses were confirmed by RT-PCR and sequencing. Titers of viral stocks were determined by plaque assay in MDCK cells.

**siRNA mediated Knockdowns**

Cells were transfected using Lipofectamine™ RNAiMAX Transfection Reagent (Invitrogen) according to the manufacturer's instructions. Cells were transfected with siRNA pools targeted to either human PAF1 (L-020349-01, Dharmacon), CHD1 (L-008529-00, Dharmacon) or a control non-targeting pool (D-001810-10-05, Dharmacon) at a final siRNA concentration of 50 nM. Transfected cells were used for further assays at 48 hours post transfection and gene knockdown efficiency was determined by quantitative PCR and/or Western blotting.

The sequences for the pooled human CHD1 siRNA oligonucleotides are as follows:

CACAAGAGCUGGAGGUCUA

GAUGAAGAUUGGCAAAUGU

CGAUCUCAUUUCUGAAUUA

GUACCGCUCUCCACUCUUA

The sequences for the pooled human PAF1 siRNA oligonucleotides are as follows:

GUGCCAUGGAUGCGAAAGA

GAGUACAACUGGAACGUGA

CUGUAGAAGAGACGUUGAA

CCACUGAGUUCAACCGUUA

**Preparation of RNA-sequencing (RNA-Seq) libraries**

RNA-Seq libraries were prepared with a protocol adapted from reference [54]. Briefly, total RNA was extracted from infected A549 cells at different time points post infection using Trizol reagent (Invitrogen). Ribosomal RNA was depleted using the RiboMinus™ Eukaryote Kit for

RNA-Seq (Invitrogen). Prior to fractionation, RNA was also treated with RNase-free DNase I (Qiagen) and purified using the RNeasy MinElute kit (Qiagen).

The RNA was fractionated in fragmentation buffer (40mM Tris acetate, pH8.2, 100mM potassium acetate and 30mM magnesium acetate) at 94 °C for 4.5 min. The fragmented RNA was reverse transcribed (Superscript III, Invitrogen) and then purified using the QIAGEN QIAquick PCR purification kit. The complementary DNA (cDNA) was then end-repaired using T4 DNA polymerase (NEB), DNA polymerase I, Large (Klenow) Fragment (NEB) and T4 PNK (NEB). End-repaired DNA was purified using the QIAGEN Quiaquick PCR purification kit. Klenow Fragment (NEB) was used to add 'A' bases to the 3'end of the DNA fragments before being purified by the QIAGEN MinElute PCR purification kit. Sequencing adaptor oligonucleotides (Illumina) were added with T4 DNA Ligase (NEB). Double-stranded cDNA libraries were then separated by electrophoresis through a 2% agarose gel, and fragments ranging from approximately 175 nt to 225 nt were excised and amplified by PCR with linker-specific primers (Illumina). The integrity and quality of RNA and cDNA were monitored throughout on the Agilent Bioanalyzer 2100. Ultra-high-throughput sequencing was performed on the Illumina Genome Analyzer II (GAII) by standard sequencing-by-synthesis reaction for 36-nt reads.

**Immunofluorescence**

A549 cells were cultured on coverslips overnight and then infected with the virus strains specified. At the indicated interval post-infection, cells were fixed in 3% paraformaldehyde (EMS) for 10 min at room temperature. Coverslips were washed in 1x PBS and blocked with blocking solution (1mg/ml BSA, 3% FBS, 0.1% Triton X100 and 1mM EDTA pH 8.0 in PBS)

for 30 min at room temperature. Cells were then probed with mouse monoclonal antibody against NS1 (diluted 1:300), or mouse monoclonal anti-Flag antibody (diluted 1:300) for 1 hr and detected by Alexa 594 conjugated Goat anti-mouse antibodies (Invitrogen). DNA was counterstained with DAPI.

**Gene Expression Analysis by Microarray**

Cells were infected with a virus strain that lacks NS1 (PR8/ΔNS1) at MOI 1 or stimulated with recombinant human IFN beta 1a (IFNβ1) (11415-1, PBL Interferon Source). Where cells were stimulated with IFNβ1, a concentration of 500 units/mL of cytokine was used. For infections with wild-type H1N1 influenza virus, the A/Puerto Rico/8/1934 (H1N1) strain was used at MOI 3. Infections with vesicular stomatitis virus (Indiana strain) were done at MOI 3. For Poly(I:C) stimulations, cells were transfected with Poly(I:C) at a final concentration of 2 μg/ml using the Lipofectamine2000 reagent (Invitrogen). Total RNA was isolated from infected, IFNβ1 stimulated or Poly(I:C) stimulated siRNA treated A549 cells using the RNeasy Kit (QIAGEN). 200ng of total RNA per sample was used to prepare biotin-labeled RNA using MessageAmp™ Premier RNA Amplification Kit (Applied Biosystems) and hybridized to HumanHT-12 v4 Expression BeadChips (Illumina). Data analysis was performed using the GeneSpring GX11.0 software (Agilent Technologies). Raw expression values were subjected to quantile normalization, and baseline transformation was performed to either the median of control samples for fold change analyses (see below), or to the median of all samples for comparisons between unstimulated siRNA treated cells.

To compare gene expression in siPAF- and control siRNA-treated cells, the normalized signal intensities of each microarray probe in the stimulated (infected or IFNβ1 stimulated) samples

was paired with and subject to baseline transformation against that of the corresponding un-stimulated sample that had been subject to the same siRNA treatment. An analysis of variance test (ANOVA) ($p < 0.001$), followed by a post hoc (TUKEY HSD) test and the indicated fold change cut offs were applied to identify probe-sets that showed statistically significant differences in expression upon stimulation for each siRNA treatment. Stimulation induced genes were defined as genes that are induced ≥2 fold ($p < 0.001$) in virus infected cells compared to un-stimulated cells in at least one siRNA treatment. hPAF1 dependent genes in virally infected and Poly(I:C) stimulated cells were defined as genes in which siPAF treatment induced a lower or greater (≥ 2 fold, $p < 0.001$) magnitude of response compared to siCtrl treated cells upon stimulation. hPAF1-dependent genes in IFNβ1-stimulated cells were defined as genes in which siPAF treatment induced a lower or greater (≥ 1.5 fold, $p < 0.001$) magnitude of response compared to siCtrl-treated cells upon stimulation. All p-value computations were subjected to multiple testing correction using the Benjamini Hochberg method.

Hierarchical clustering[55] of data was performed and visualized using the Cluster and Treeview software (http://www.eisenlab.org/eisen/). Genes that are represented by multiple probesets on the microarray are depicted by the average of those probesets in the heatmaps generated.

Functional analyses were conducted through the use of Ingenuity Pathways Analysis (Ingenuity® Systems, www.ingenuity.com). The Functional Analysis identified the biological functions that were most significant to gene lists generated from the microarray. Right-tailed Fisher's exact test was used to calculate a p-value determining the probability that each biological function assigned to that data set is due to chance alone.

**Quantitative Real-Time PCR (qPCR)**

Total RNA from stimulated cells was extracted using the RNeasy kit (QIAGEN) according to the manufacturer's instructions. RNA was DNase treated using the RNase free DNase kit (QIAGEN) and cDNA was synthesized using the First strand cDNA synthesis kit (Roche). qPCR was performed using SYBR green (Roche) or the LightCycler 480 Probes Master mix (Roche). Primer sequences are available upon request.

### *In vitro* methylation assay

Methylation assays were performed as previously described[56] with minor variations. In brief, ~300 ng of protein/peptide substrate and ~100 ng of HMTs were incubated with [$^3$H] SAM in HMT buffer (50 mM Tris-HCl (pH 8.5), 5 mM $MgCl_2$, 2 mM DTT) for 30 minutes at 37°C. The reaction was then immunoprecipitated for 1 hour with avidin beads (for experiment with peptides substrate) or GST beads (for experiments with GST substrate) and then washed extensively in BC150. This step minimizes non-specific radioactive incorporation. Eluted material was then subjected to PAGE, gel drying and exposed for radioactive signal detection. Set7/9 was a kind gift from Dr. Marc-Werner Dobenecker and purified Set1C was a kind gift from Dr. Tang Zhanyun.

### *In vitro* acetylation assay

HAT reactions were performed in HAT assay buffer (50 mM Tris at pH 8.0, 10% glycerol, 50 mM KCl, 0.1 mM EDTA, 10 mM butyric acid, 1 mM dithiothreitol [DTT], 1 mM phenylmethylsulfonyl fluoride [PMSF]). Protein/peptide substrate (~ 100ng) was incubated with [$^3$H]acetyl coenzyme A (CoA) and purified TIP60 (a kind gift from Dr. Xiao-Jian Sun) for 1h

and affinity purified using analogous immunoprecipitation of the substrate before PAGE and detection on autoradiography film (see *in vitro* methylation assay).

**Immunoprecipitation**

Nuclear extracts from untreated and infected cells (pretreated with HDAC inhibitors when required) were denatured in Laemmli buffer (63mM Tris HCl, 10% Glycerol, 2% SDS, pH6.8) at 95°C for 10 minutes (with cycles of vortexing). The extract was then diluted to a final concentration of 0.2%SDS in BC150 and sonicated with a Bioruptor (Diagenode). Proteins were then immunoprecipitated with Flag M2 antibody (Sigma)-coupled magnetic beads for 2 hours at 4°C. After extensive washing in BC300 and BC150 (last wash), the material was eluted with Flag-competing peptide at 37°C for 15 minutes (3 cycles) and the eluted material was combined and acetone-precipitated. Western blotting for NS1 modifications was followed by stripping and re-probing for loading control.

**Peptides pull-down assays**

Pull-down assays with extracts and recombinant proteins were performed as described previously[57]. Nuclear extracts were prepared from HEK293 cells using the Dignam protocol[58]. Briefly, $10^8$ cells were used per pull-down assay. Salt and Triton-X100 concentrations were 250mM and 0.2% (v/v), respectively. Fractions from nuclear extracts fractionated on Heparin column, were precleared with avidin beads and then incubated with biotinylated-peptide prebound to avidin beads for 3h at 4°C. Approximately 2µg of peptide was used per pull down. Beads were washed eight times with BC300 containing protease inhibitor cocktail (Roche). Bound proteins were eluted from the resin using 100mM glycine, pH2.8 and run on Micro-Spin

Columns (Pierce, 89879). Eluates were combined, neutralized, and analyzed by SDS–PAGE. A similar procedure was used for peptide pull down using purified protein (100ng) or reconstituted complex (1µg). All peptides were synthesized by the Rockefeller University Proteomics Resource Center.

**Antibodies**

Anti-dimethyl NS1 antibody (NS1me2) was raised in rabbits against peptides (220-230) bearing pre-methylated K229 residue. Methyl specific antibodies were purified first by pre-absorbing serum (1 out of 8 rabbits showed highly reactive methyl-specific serum at the second bleed after peptide injection) to a matrix containing unmodified peptides, followed by purification on a NS1me2 column. Anti-PB1 and anti-NP are custom made antibodies kindly provided by P. Palese. Mouse anti-Flag is from Sigma (A8592); antibody against hPAF1C subunits were all purchased from Bethyl laboratories: PAF1 (A301-047A); CTR9 (A301-385A); LEO1 (A310-048A); RTF1 (A300 179A); Parafibromin/CDC73 (A300-170A); as well as CHD1(A301-218) and SMARCAL1(A301-086). Anti-H3K4me3 was purchased from Millipore (17-614), while Anti-RNA Pol II CTD (Ab5408) was purchased from Abcam. GST antibody was from Roche (RPN1236V).

**Differential salt extraction**

Defined numbers of A549 cells were seeded and subsequently infected with influenza virus. Nuclear proteins were extracted at increasing concentrations of NaCl from 10 mM up to 2 M in BC buffer. Eluted materials were resolved on PAGE and immunoblotted with specific antibody.

**Chromatin-immunoprecipitation**

We used a slightly modified version of described protocols to perform crosslinking ChIP[59,60]. Both protocols use Invitrogen Dynal magnetic beads (Invitrogen Dynabeads anti-mouse M-280 #112-02, or Dynabeads anti-rabbit M-280 #112-04, or Dynabeads Protein A #100-02D). Untreated or influenza infected A549 cells were fixed with 1% paraformaldehyde. Approximately 10 million cells were used for each ChIP (5 times more material was used for Flag assay due to reduced performances of anti-Flag antibody on cross-linked material). For sonication, we used a Bioruptor (Diagenode) and optimized sonication conditions to generate DNA fragments of approximately 300-500 bp. Following the x-link ChIP protocol from Lee[60] through overnight crosslink reversal at 65°C, we collected immunoprecipitated protein complexes and analyzed them via PAGE, or alternatively, we isolated ChIP DNA after RNase digestion and proteinase K digestion.

**ChIP-Sequencing**

For ChIP-Seq of x-link ChIP DNA, we took 30ul of ChIP DNA, repaired DNA ends to generate blunt-ended DNA using the Epicenter DNA ENDRepair kit (Epicenter Biotechnologies, cat# ER0720), and purified end-repaired DNA using the QIAGEN PCR purification kit (28104). Following DNA END Repair, we added A bases to the 3′ end of the DNA fragments using Klenow Fragment (NEB M0212L), and purified DNA using the QIAGEN MinElute kit (28004). We ligated Illlumina/Solexa adapters (#FC-102-1003) to DNA fragments overnight, using T4 DNA ligase (NEB M0202L). Following overnight ligation, we purified adaptor-ligated DNA fragments with the QIAGEN MinElute kit. To generate libraries for Solexa sequencing, we performed 18 cycles of PCR with Illumina/Solexa primers 1.0 and 2.0, checked the fragment size

for 1/10 of our amplified library on an agarose gel, and purified the remaining ChIP-seq library using the QIAGEN MinElute kit. The purified DNA was used for cluster generation on Illumina/Solexa flow cells, and sequencing analysis was performed on an Illumina/Solexa Genome Analyzer 2 following manufacturer protocols.

**GRO-sequencing**

Transcriptionally active nuclei from infected or untreated A549 cells were prepared after swelling for 5 minutes the cells in ice-cold swelling buffer (10mM Tris (pH = 7.5), 2mM $MgCl_2$, 3mM $CaCl_2$). Pelleted cells were resuspended in 1ml lysis buffer (10mM Tris (pH = 7.5), 2 mM $MgCl_2$, 3mM $CaCl_2$, 10% glycerol, 0.5% NP40, 2U/$ml^{-1}$ SUPERaseIN (Ambion) and pipetted 20 times with a P1000 tip with the end cut off to reduce shearing. Volume was brought to 10 ml with lysis buffer and nuclei were pelleted at 600*g* for 5min. Nuclei were washed in 10ml lysis buffer and re-pelletted. A small aliquot was taken for Trypan blue staining to check that lysis occurred and nuclei were still intact. Nuclei were resuspended in 1ml freezing buffer (50mM Tris-Cl (pH = 8.3), 40% glycerol, 5mM $MgCl_2$, 0.1mM EDTA) using a P1000 tip with the end cut off and re-pelletted and re-resuspended in 500µl of freezing buffer and aliquoted into 100µl aliquots and frozen in liquid nitrogen.

GRO-Seq libraries were prepared as described previously[61].

SSPE, NaCl, KCL, EDTA, and water are DEPC treated, while SDS, Sarkosyl, DTT, Tween, Tris buffers, PVP, NaOH were made with DEPC treated water, then filter-sterilized. Buffers used for immunoprecipitation contain superRNAsIN (1µl per 5 ml buffer) (Ambion) to block degradation that can occur during the experimental procedure.

**Proteins and complex purifications**

Baculoviruses were generated according to the manufacturer's instruction (GIBCO-Invitrogen). Sf9 cells were infected with combinations of baculoviruses and proteins/complexes were affinity purified on M2 agarose[62].

**Transcription Assay**

In vitro transcription was done as previously described[63]. In brief, we used an *in vitro* transcription assay containing highly purified transcription factors (Pol II, TFIID, TFIIA, TFIIB, TFIIE, TFIIF, TFIIH, PC4, and Mediator) and a pML array template that contains p53-binding sites nearby the core promoter and generates 390-nucleotide transcription products. This system previously was shown to effect activator-dependent transcription[63].

**Sequencing**

Samples were sequenced in accordance with manufacturer protocols on GAIIx and HiSeq2000 instruments. Image data was analyzed in real-time by the onboard RTA software package.

**Raw Data Analysis**

Bcl files produced by RTA were converted to qseq files by Illumina’s OLB software package, and qseq files converted to fastq for subsequent analysis.

**ChIP-Seq Alignments**

Sequencing reads were aligned to the Human March 2006 (NCBI36/hg18) assembly using the short-read aligner Bowtie[64]. Reads were aligned at 36bp allowing for 2 mismatches to the reference, reporting unique alignment locations only. RefSeq annotation data was downloaded from the UCSC table browser.

**RNA-Seq Analysis**

Sequencing reads were processed using Tophat[65], a junction mapping alignment program designed to identify splice junctions from RNA-Seq reads. Briefly, the program aligns reads to a reference genome, identifying regions of coverage that correspond to transcribed RNA. The underlying sequence of adjacent regions is joined together to create a spliced reference, and reads that did not initially align to the reference genome are aligned to identify sequencing reads that originated from potential splice junctions (e.g. exon-exon junctions).The Cufflinks[66] software package was used to perform gene expression level calculations and comparisons between RNA-Seq libraries prepared from uninfected cells and infected cells.

**GRO-Seq Analysis**

All sequencing reads were 51bp long. Reads that passed the internal Illumina quality filter were processed for adapter trimming, and reads which were longer than 15bp after adapter removal were retained. This subset of reads was aligned allowing 2 mismatches to the reference. Reads which were not trimmed of adapter sequence were truncated by 6bp at the 3'end to allow for potential incomplete adapter trimming, and aligned allowing 3 mismatches to the reference. Duplicate alignment positions were condensed to a single alignment entry to account for potential amplification biases. The adapter-trimmed and no-adapter alignments were merged for

all subsequent analyses. All reads were aligned using the short-read aligner bowtie to the Human March 2006 (NCBI36/hg18) assembly.

Strand-specific coverage files were generated to differentiate between sense and antisense transcripts and to facilitate proper assignment of enrichment information for gene profiling.

GRO-Seq FPKM values were obtained by calculating the number of reads in the transcriptional unit and reporting per kilobase of gene length per million mapped reads.

Integrated profiles (see the following Integrated ChIP-profile) were made reflecting 3kb upstream from the TSS and 3kb downstream from the TES and 300 internal windows.

1000 genes were selected randomly from a group of 16,806 genes that had similar gene body enrichment level ranges relative to genes in Table 2. The GRO-Seq data from WT 12H was used for this selection.

**Integrated ChIP-Seq profiles**

Genes were profiled 2.5kb upstream of the TSS, through the gene body and 2.5kb downstream of the transcriptional end site (TES). Read counts were calculated in 100bp windows up and downstream of the TSS and TES, and each gene was segmented in 300 internal windows. Plots were made using a 1kb moving average. Values are read-normalized and reflect the number of reads observed in each averaged window.

Genes were selected by requiring a log2 fold-change increase in expression of greater than 2, PolII-Total ChIP-Seq enrichment increase throughout the gene body (600bp downstream of the TSS to 3kb downstream of the TES) of greater than >1.4-fold at 12 hours post infection compared to uninfected cells, and an H3K4me3 peak in either uninfected cells or cells 12 hours post-infection (as determined by MACS[67] using custom settings for H3K4me3) within 3kb of the

TSS. Additionally, genes passing these criteria were filtered out if the TES of genes with higher than 2 FPKM within 10kb of their TSS in an effort to minimize the effect of high RNA Pol II at the TES of highly transcribed genes.

For NS1 ChIP-Seq in A549 infected siPAF1, siCHD1 and siCtrl conditions, enrichment data was calculated for all RefSeq genes 5kb +/- TSS in 50bp windows, and anti-Flag ChIP-Seq enrichment values from uninfected cells was calculated similarly and subtracted. Values are read-normalized and reflect the number of reads observed in each window.

**References**


51 Varble, A. *et al.* Engineered RNA viral synthesis of microRNAs. *P Natl Acad Sci USA* **107**, 11519-11524, doi:DOI 10.1073/pnas.1003115107 (2010).

52 Quinlivan, M. *et al.* Attenuation of equine influenza viruses through truncations of the NS1 protein. *J Virol* **79**, 8431-8439, doi:Doi 10.1128/Jvi.79.13.8431-8439.2005 (2005).

53 Fodor, E. *et al.* Rescue of influenza A virus from recombinant DNA. *J Virol* **73**, 9679-9682 (1999).

54 Rosenberg, B. R., Hamilton, C. E., Mwangi, M. M., Dewell, S. & Papavasiliou, F. N. Transcriptome-wide sequencing reveals numerous APOBEC1 mRNA-editing targets in transcript 3' UTRs. *Nat Struct Mol Biol* **18**, 230-236, doi:nsmb.1975 [pii] 10.1038/nsmb.1975 (2011).

55 Eisen, M. B., Spellman, P. T., Brown, P. O. & Botstein, D. Cluster analysis and display of genome-wide expression patterns. *Proc Natl Acad Sci U S A* **95**, 14863-14868 (1998).

56 Nishioka, K. *et al.* PR-Set7 is a nucleosome-specific methyltransferase that modifies lysine 20 of histone H4 and is associated with silent chromatin. *Mol Cell* **9**, 1201-1213 (2002).

57 Wysocka, J. Identifying novel proteins recognizing histone modifications using peptide pull-down assay. *Methods* **40**, 339-343, doi:DOI 10.1016/j.ymeth.2006.05.028 (2006).

58 Dignam, J. D., Lebovitz, R. M. & Roeder, R. G. Accurate Transcription Initiation by Rna Polymerase-Ii in a Soluble Extract from Isolated Mammalian Nuclei. *Nucleic Acids Res* **11**, 1475-1489 (1983).

59 Barski, A. *et al.* High-Resolution Profiling of Histone Methylations in the Human Genome. *Cell* **129**, 823-837 (2007).

60 Lee, T. I., Johnstone, S. E. & Young, R. A. Chromatin immunoprecipitation and microarray-based analysis of protein location. *Nat Protoc* **1**, 729-748, doi:Doi

61 Core LJ. et al. Nascent RNA sequencing reveals widespread pausing and divergent initiation at human promoters. Science. 2008 Dec 19;322(5909):1845-8. Epub 2008 Dec 410.1038/Nprot2006.98 (2006).

62 Kim, J., Guermah, M. & Roeder, R. G. The Human PAF1 Complex Acts in Chromatin Transcription Elongation Both Independently and Cooperatively with SII/TFIIS. *Cell* **140**, 491-503, doi:DOI 10.1016/j.cell.2009.12.050 (2010).

63 Guermah, M., Palhan, V. B., Tackett, A. J., Chait, B. T. & Roeder, R. G. Synergistic Functions of SII and p300 in Productive Activator-Dependent Transcription of Chromatin Templates. *Cell* **125**, 275-286 (2006).

64 Langmead, B., Trapnell, C., Pop, M. & Salzberg, S. L. Ultrafast and memory-efficient alignment of short DNA sequences to the human genome. *Genome Biol* **10**, doi:10.1186/gb-2009-10-3-r25 (2009).

65 Trapnell, C., Pachter, L. & Salzberg, S. L. TopHat: discovering splice junctions with RNA-Seq. *Bioinformatics* **25**, 1105-1111, doi:10.1093/bioinformatics/btp120 (2009).

66 Pachter, L. *et al.* Transcript assembly and quantification by RNA-Seq reveals unannotated transcripts and isoform switching during cell differentiation. *Nat Biotechnol* **28**, 511-U174, doi:10.1038/nbt.1621 (2010).

67 Li, W. *et al.* Model-based Analysis of ChIP-Seq (MACS). *Genome Biol* **9**, doi:10.1186/gb-2008-9-9-r137 (2008).